Odovtos-International Journal of Dental Sciences (Odovtos-Int. J. Dent. Sc.) 28 (2), 2026 (May-August): 231-245. SSN: 2215-3411
https://doi.org/10.15517/n6y6a095

ODOVTOS
International Journal of Dental Sciences

UNIVERSIDAD DE COSTA RICA FOd Facultad de Odontología

https://revistas.ucr.ac.cr/index.php/rOdontos

BASIC RESEARCH:

Biocompatibility, Cytotoxicity, and Antibacterial Evaluation of Novel Chitosan-Based 3D Bioprinted Bone Scaffolds: *In Vitro* Study

Evaluación de la biocompatibilidad, citotoxicidad y actividad antibacteriana de nuevos andamios óseos bioimpresos en 3D a base de quitosano: estudio *in vitro*

Parkavi Arumugam MDS[1] https://orcid.org/0000-0001-5771-8994
Dhivya Sarathi[2] https://orcid.org/0009-0008-2495-3443
Kaarthikeyan Gurumoorthy MDS, PhD[3] https://orcid.org/0000-0002-5521-7157
Ramanarayana Boyapati MDS[4] https://orcid.org/0000-0002-9196-0183

[1]Associate Professor, Department of Periodontics, Saveetha Dental College and Hospitals, Saveetha Institute of Medical and Technical Sciences, Saveetha University, Chennai, India.
[2]Graduate student, Saveetha Dental College and Hospitals, Saveetha Institute of Medical and Technical Sciences, Saveetha University, Chennai, India.
[3]Professor, Department of Periodontics, Saveetha Dental College and Hospitals, Saveetha Institute of Medical and Technical Sciences, Saveetha University, Chennai, India.
[4]Professor, Department of Periodontology, Sibar Institute of Dental Sciences, Guntur, India.

Correspondence to: Dr. Parkavi Arumugam, MDS - parkavia.sdc@saveetha.com

Received: 28-IX-2025 Accepted: 9-I-2026

ABSTRACT: The objective of the study was the biologic characterisation of novel three dimensional (3D) bioprinted osseous scaffolds developed for bone tissue engineering, using biocompatibility, cytotoxicity analysis and antibacterial assay. A composite bioink comprising polyethylene glycol (PEG), polyethylene glycol diacrylate (PEGDA), hydroxyapatite (HAP), collagen (COL), and chitosan (CH)was formulated and 3D bioprinted into osseous scaffolds using Cellink Bio X, extrusion-based 3D bioprinter. *In vitro* biologic characterisation included 3-(4,5-Dimethylthiazol-2-yl)-2,5-diphenyltetrazolium bromide (MTT) assay for biocompatibility using MG-63 osteoblast-like cells, cytotoxicity analysis using zebrafish model, with Group A (3D bioprinted scaffolds) and Group B (Phosphate buffer saline). Antibacterial assay was performed using disc diffusion method, with Group A1(low concentration of 3D bioprinted scaffolds), Group A2 (high concentration of 3D bioprinted scaffolds), Group B (dimethyl sulfoxide), and Group C (20 mg Erythromycin and 20 mg Penicillin) against *Staphylococcus aureus* (*S. aureus*, MTCC 740), *Streptococcus mutans* (*S. mutans*, MTCC 890), *Enterococcus faecalis* (*E. faecalis*, MTCC 439), and *Klebsiella pneumoniae* (*K. pneumoniae*, MTCC 109). Biologic characterisation revealed good biocompatibility of Group A (3D bioprinted scaffolds) comparable to Group B (untreated MG63), at all time points. No significant difference in embryo viability was observed for both Groups A and B, with good length, prominent trunk, tail, and organ development. Antibacterial assay revealed significant intergroup activity across all tested

strains (p=0.000), with comparable zone of inhibition of Group A2 with the control against *S. aureus* and *S. mutans*. The biologic characterization of the novel 3D bioprinted osseous scaffolds revealed good biocompatibility, limited cytotoxicity, and promising antibacterial properties. These findings underscore the potential of the developed constructs for application in bone tissue engineering for enhancing overall health. Future studies should focus on osteogenic differentiation, mineralization, and *in vivo* performance.

KEYWORDS: Three-dimensional bioprinting; Tissue engineering; Bone regeneration; Collagen; Chitosan; Hydroxyapatite; Health.

RESUMEN: El objetivo del estudio fue la caracterización biológica de nuevos andamios óseos tridimensionales (3D) bioimpresos, desarrollados para ingeniería de tejidos óseos, mediante análisis de biocompatibilidad, citotoxicidad y ensayo antibacteriano. Se formuló una biotinta compuesta por polietilenglicol (PEG), diacrilato de polietilenglicol (PEGDA), hidroxiapatita (HAP), colágeno (COL) y quitosano (CH), la cual fue bioimpresa en 3D para obtener andamios óseos utilizando una bioimpresora 3D de extrusión Cellink Bio X. La caracterización biológica *in vitro* incluyó el ensayo de 3-(4,5-dimetiltiazol-2-il)-2,5-difeniltetrazolio bromuro (MTT) para evaluar la biocompatibilidad utilizando células osteoblásticas tipo MG-63, el análisis de citotoxicidad mediante un modelo de pez cebra, con el Grupo A (andamios bioimpresos en 3D) y el Grupo B (solución salina tamponada con fosfatos). El ensayo antibacteriano se realizó mediante el método de difusión en disco, con el Grupo A1 (baja concentración de andamios bioimpresos en 3D), el Grupo A2 (alta concentración de andamios bioimpresos en 3D), el Grupo B (dimetilsulfóxido) y el Grupo C (20 mg de eritromicina y 20 mg de penicilina), frente a *S. aureus*, *S. mutans*, *E. faecalis* y *K. pneumoniae* . La caracterización biológica reveló una buena biocompatibilidad del Grupo A (andamios bioimpresos en 3D), comparable al Grupo B (MG-63 no tratadas), en todos los tiempos evaluados. No se observaron diferencias significativas en la viabilidad embrionaria entre los Grupos A y B, evidenciándose una adecuada longitud, un tronco prominente, cola bien definida y desarrollo adecuado de órganos. El ensayo antibacteriano mostró una actividad intergrupal significativa frente a todas las cepas evaluadas (p=0.000), con zonas de inhibición del Grupo A2 comparables a las del grupo control frente a *S. aureus* y *S. mutans*. La caracterización biológica de los nuevos andamios óseos bioimpresos en 3D demostró una buena biocompatibilidad, citotoxicidad limitada y propiedades antibacterianas prometedoras.

PALABRAS CLAVE: Bioimpresión tridimensional; Ingeniería de tejidos; Regeneración ósea; Colágeno; Quitosano; Hidroxiapatita; Salud.

INTRODUCTION

Intraoral bone defects resulting from periodontal disease, trauma, and pathologies remain the most common conditions requiring rehabilitative approaches to restore the form and function of the lost tissues. Tooth loss that presents as a sequel requires considerable prosthodontic measures, such as fixed dentures and implants, to replace the lost teeth. However, insufficient bone levels often complicate the placement of implants. Although various surgical, bone grafting, and tissue engineering techniques have been employed to overcome these issues, achieving complete and predictable bone regeneration remains elusive. With the advances in additive manufacturing technology, the emergence of three-dimensional (3D) bioprinting has revolutionised the field of tissue engineering and regenerative medicine. Based on the components of tissue engineering, the employment of cells, scaffolds, and growth factors has enabled the bioprinting of tissue scaffolds in a layer-by-layer manner (1). Moreover, the bioprinted scaffolds are fabricated according to the dimensions of the tissue defects, allowing for greater precision and control over the spatial micropatterns, enabling personalised treatment approaches (2).

Among the bioprinting technologies available, extrusion-based bioprinting is the most conducive for the printing of tissue scaffolds, with the extrusion of the bioink as a thin filament (3). Bioink lies at the core of this technology, due to its directive effect on the compositional, structural, and functional behavior of printed scaffolds (4). These inks are designed to support cell growth, provide biomimicry, and culminate in the regeneration of functional tissues. Bioinks are typically classified into two broad categories: cell-based bioinks, which include living cells along with biomaterials, and biomaterial-based bioinks, which are devoid of living cells but contain various biomaterials that support the growth and differentiation of cells *in vitro* (5). The selection and development of bioinks are critical for advancing the capabilities of 3D bioprinting and realising its full potential in medical and research applications.

The primary goal of cell-based bioinks is to provide an environment that supports cell viability throughout the bioprinting process and post-printing tissue maturation. This requires carefully controlled rheological properties that allow the bioink extrusion while causing minimal shear stress on cells and maintaining its shape fidelity after deposition (6). Additionally, bioinks must have tunable degradation rates that are in accordance with the regenerative rate of the new tissues. Challenges related to cell-based bioinks include ensuring high cell density, viability, and mechanical properties while minimising contamination and addressing issues of vascularisation within printed tissues. Developing techniques to enable nutrient and oxygen delivery to cells deep within thick tissue constructs remains a significant hurdle.

Biomaterial-based bioinks are primarily composed of natural and synthetic biocompatible materials like collagen (COL), alginate, chitosan (CH), hyaluronic acid, and polyethylene glycol (PEG), Polyethylene glycol diacrylate (PEGDA), polylactic acid (PLA), polycaprolactone (PCL), hydroxyapatite (HAP), and bioglass (BG), respectively. Natural materials provide biomimicking cues while synthetic materials enhance the mechanical properties of the constructs (7). However, a balance between these natural and synthetic components is essential to create bioinks that are both biologically functional and mechanically robust. Although these biomaterial-based inks do not contain cells initially, they can be combined with post-printing cell seeding or treatment in bioreactors to promote cellular growth (8). Their main advantage lies in the easier handling, longer shelf life, and a larger scope for customisation according to the needs.

In the present study, we developed a composite bioink composed of PEG-PEGDA-HAP-COL-CH for the bioprinting of osseous scaffolds. The printed scaffolds were then characterised for biocompatibility, cytotoxicity, and antimicrobial properties, to assess their clinical compatibility for bone tissue engineering applications.

MATERIALS AND METHODS

The study was conducted at the Department of Biomaterials, Saveetha Dental College and Hospitals, India. Approval for the conduction of the study was obtained from the Institutional Scientific Review Board with approval number: SRB/SDC/UG-2033/24/PERIO/470. All the chemicals and biomaterials used were of analytical grade and sourced from Sigma-Aldrich. HAP nanoparticles were sourced from Nano Research Lab, India. MG-63 cells were sourced from the National Centre for Cell Science, Pune, India. Zebra fish embryos were sourced from a local vendor in Chennai. Single blinding was implemented wherein the investigator performing the experiments and measurements was unaware of group allocation to minimize observational bias.

BIOINK FORMULATION

A composite bioink was formulated by combining PEG, PEGDA, HAP, COL, and CH. The process started with the dissolution of CH (1%w/v) in 1% acetic acid for 4-6 hours. The pH was then maintained at 7 to 7.4 by adding 0.1 N sodium hydroxide (NaOH) and stirring constantly. PEG 4000 (20% w/v) flakes were mixed with PEGDA (65% w/v) polymer under gentle heating at 40-50°C. The CH solution was then introduced into the mixture, resulting in a blended formulation. To this mixture, HAP (13% w/v) nanoparticles and marine origin COL (1% w/v) powder were added at room temperature and sonicated to obtain a homogenous dispersion. A photoinitiator solution composed of camphorquinone (0.5% w/v) and ethyl 4-dimethylaminobenzoate (0.2% w/v) in 100 µl absolute ethanol was added to the bioink under light-protective conditions and stored at 4°C until further use.

3D BIOPRINTING OF THE OSSEOUS SCAFFOLDS

Cellink extrusion-based bioprinter Bio X was used for the bioprinting of scaffolds. The bioink was extruded using an 18-gauge nozzle at a pressure of 12 KPa at a speed of 4mm/sec at room temperature. Scaffolds were printed as a 20mm*20mm*4mm grid with 50% infill, with each layer having a height of 1mm. The printed scaffolds were then light-cured at 460 nm. Biologic characterisation of the scaffolds was done by performing biocompatibility, cytotoxicity and antibacterial analysis.

BIOCOMPATIBILITY ANALYSIS

The biocompatibility of sterilised 3D-bioprinted scaffolds was evaluated using the 3-(4,5-Dimethylthiazol-2-yl)-2,5-diphenyltetrazolium bromide assay (MTT) assay to determine cell viability on MG63 osteoblast cell line. 3D bioprinted scaffolds (Group A) were considered as test group. The scaffolds were sectioned into fragments measuring 5mm×5mm×2mm and immersed in alpha-modified Minimum Essential Medium (α-MEM) supplemented with 1% antibiotic solution and incubated for 24 hours. Following incubation, the extract was collected and filtered to remove any particulates and utilised as the treatment medium for Group A. Untreated MG63 cells (Group B) were set as the control. MG63 cells were seeded at a density of 0.05 × 106^66 cells per well and treated with the prepared treatment medium. After 24 hours of treatment, the MTT assay was conducted. The spent medium was removed, and MTT reagent was added to each well. The plates were incubated at 37°C for four hours to allow the formation of formazan crystals. Subsequently, the MTT reagent was replaced with

dimethyl sulfoxide (DMSO) to dissolve the formazan crystals. Absorbance was measured at 570 nm using an enzyme-linked immunosorbent assay (ELISA) plate reader. All tests were performed in triplicate, and the percentage of cell viability was calculated and compared for Groups A and B.

CYTOTOXICITY ANALYSIS

The zebrafish model was utilised to evaluate the cytotoxicity of the 3D-bioprinted scaffolds. The 3D bioprinted scaffold (Group A) was considered the test group, while E3 embryo culture medium (Group B) was set as the control. The scaffold was cut into small pieces, and 100 mg of scaffold material was immersed in 10 ml of PBS. The solution was incubated at 37°C for 24-72 hours under static conditions to allow the leaching of soluble components. The scaffold extract containing the leachates was collected, filtered to remove any particulate matter, and introduced to a suspension containing the zebrafish embryos. Approximately 25 zebrafish embryos were carefully maintained at optimal temperature and monitored at specific time intervals for the development of organs such as head, tail, and eyes. The number of dead embryos was recorded and compared to the control samples. To prevent contamination of the suspension, dead embryos and fish were removed during each observation. The mortality rate was calculated at the end of every 24-hour period.

ANTIBACTERIAL ACTIVITY

The antibacterial activity of the 3D bioprinted osseous scaffolds was assessed against *Staphylococcus aureus* (*S. aureus*, MTCC 740), *Streptococcus mutans* (*S. mutans*, MTCC 890), *Enterococcus faecalis* (*E. faecalis*, MTCC 439), and *Klebsiella pneumoniae* (*K. pneumoniae*, MTCC 109) using the disc diffusion method. Group A, consisting of the 3D bioprinted scaffold extract, was considered the test group, while Group B, consisting of dimethyl sulfoxide (DMSO), was considered the negative control, and Group C, consisting of a combination of antibiotics, 20 mg Erythromycin and 20 mg Penicillin (1:1%), was considered the positive control. The 3D bioprinted scaffolds of the test Group A were further assessed at a low concentration of 20µg/ml as Group A1 and a high concentration of 40µg/ml as Group A2, to analyse the dose-response relationship and the therapeutic potential. The 3D bioprinted osseous scaffolds were cut into 5mm*5mm*2mm pieces, sterilised using UV irradiation, prior to immersion in a mixture of sterile nutrient broth and DMSO. The immersed scaffolds were incubated at 37°C for 24-48 hours under static conditions, allowing leachates to diffuse into the medium, following which the medium was filtered through Whitman filter paper to remove any particulate matter, leaving only the scaffold extract. Mueller-Hinton agar plates were prepared according to the manufacturer's instructions, and 100 µL of the bacterial suspension was evenly spread on the agar surface using a sterile swab. Sterile filter paper discs of 6mm diameter were soaked in the scaffold extract, positive and negative controls, and allowed to dry before being placed on the inoculated agar plates. This setup was then incubated at 37°C for 24 hours. The diameter of the zone of inhibition (ZOI) was measured around the discs to compare and assess the antimicrobial activity.

STATISTICAL ANALYSIS

Data were analyzed using IBM SPSS Statistics for Windows, Version XX (IBM Corp., Armonk, NY, USA). All experiments were performed in triplicates, and results are expressed as mean ± standard deviation (SD). The Shapiro-Wilk test was used to verify the normality of data distribution, and Levene's test was applied to assess the homogeneity of variances. To evaluate the effects of group (bioink composition) and time on biocompatibility and cytotoxicity of the 3D bioprinted scaffolds, a two-way analysis of variance (ANOVA) was performed, followed by Tukey's post hoc test for multi-

ple comparisons. One-way ANOVA was performed to compare the antibacterial effect of GROUP A1, GROUP A2, GROUP B, and GROUP C. A p value < 0.05 was considered statistically significant.

RESULTS

BIOCOMPATIBILITY ANALYSIS

MTT assay (Figure 1, Table 1 and Table 2) demonstrated comparable cell viability between Groups A and B at all evaluated time points. Two-way ANOVA revealed no statistically significant difference between the groups ($F=3.754$, $p=0.067$), indicating that both scaffolds exhibited similar levels of biocompatibility. A significant main effect of time was observed ($F=88.398$, $p<0.001$), suggesting expected variations in cell viability across the incubation periods. However, the interaction between group and time was not significant ($F=0.746$, $p=0.572$), confirming that both groups followed a similar pattern of change in viability over time. The highest percentage of cell viability was observed at 24 hours, with a gradual decline at later time points, which is considered a normal cellular response under *in vitro* experimental conditions. Tukey's multiple comparison test revealed that the mean percentage of cell viability at 24 hours was significantly higher than at all subsequent time points ($p<0.05$). Significant differences were also observed between most other time intervals, indicating progressive variations in cell viability over time. Specifically, the differences between 24-48 hrs, 48-72 hrs, 48-96 hrs, and 48-120 hrs were statistically significant ($p<0.05$), confirming temporal changes in cell metabolic activity under the given *in vitro* conditions. The consistent reduction in viability values observed with increasing incubation periods reflects normal cellular adaptation and metabolic decline over extended culture durations, rather than cytotoxicity. The results prove that the components used in the bioink, along with the photoinitiators, did not have any adverse effects on cell growth. Confocal analysis revealed proliferating spindle-shaped cells in layers, with viable cell nuclei that were well-appreciable. The cells also revealed extended filopodia in contact with neighbouring cells, proving the cell migratory and differentiating effect of the scaffold on the cells.

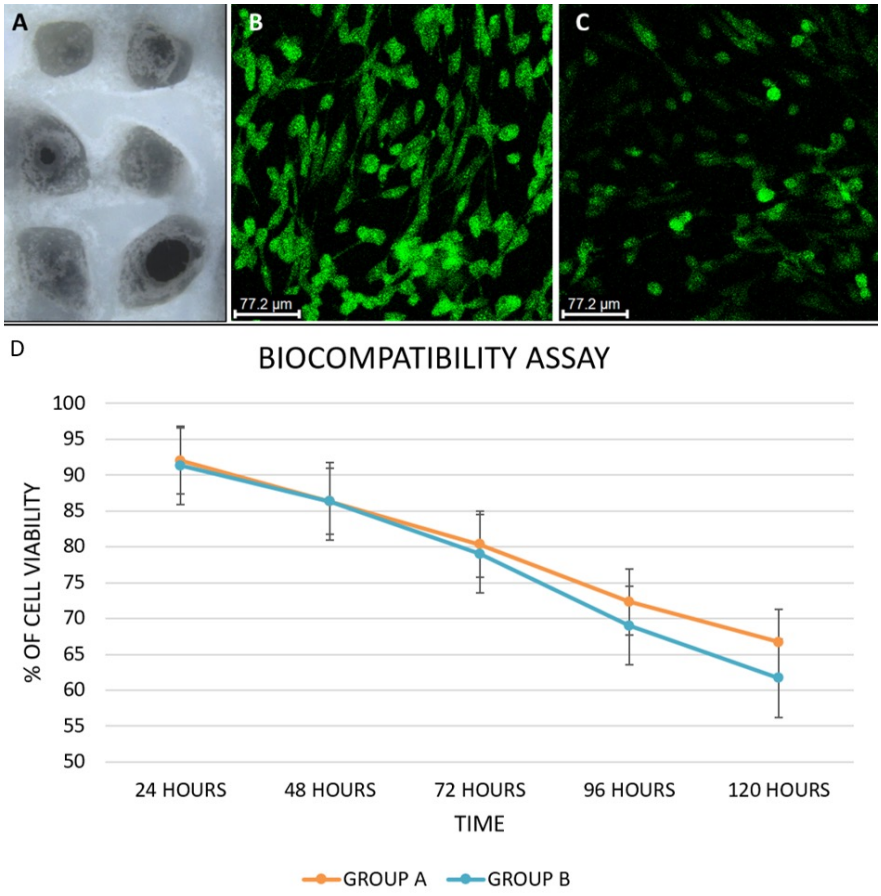

Figure 1. A: Stereomicroscopic image of the 3D bioprinted scaffold, B-C: Confocal analysis revealing viable MG63 cells for both Group A (B) and Group B (C), D: Comparative analysis of biocompatibility of Group A and B, expressed as percentage of cell viability. Cytotoxicity Analysis - Zebrafish Model.

Table 1. Comparison of biocompatibility as mean cell viability (%) between Groups A and B at different time intervals using two-way ANOVA

Time (hours)	Group A (Mean ± SD)	Group B (Mean ± SD)	F (Group)	P (Group)	F (Time)	P (Time)	F (Group x Time)	P Group x Time)
24	92.00 ± 2.00	91.33 ± 1.53						
48	86.33 ± 2.52	86.33 ± 4.51						
72	80.33 ± 2.52	79.00 ± 3.00	3.754	0.067	88.398	<0.001	0.746	0.572
96	72.33 ± 2.52	69.00 ± 3.00						
120	66.67 ± 3.51	61.67 ± 3.06						

Table 2. Tukey's post hoc comparison of biocompatibility across time intervals.

(I) Time		Mean Difference (I-J)	Sig.	95% Confidence Interval	
				Lower Bound	Upper Bound
24.00	48.00	5.3333*	.035	.2865	10.3801
	72.00	12.0000*	.000	6.9532	17.0468
	96.00	21.0000*	.000	15.9532	26.0468
	120.00	27.5000*	.000	22.4532	32.5468
48.00	24.00	-5.3333*	.035	-10.3801	-.2865
	72.00	6.6667*	.006	1.6199	11.7135
	96.00	15.6667*	.000	10.6199	20.7135
	120.00	22.1667*	.000	17.1199	27.2135
72.00	24.00	-12.0000*	.000	-17.0468	-6.9532
	48.00	-6.6667*	.006	-11.7135	-1.6199
	96.00	9.0000*	.000	3.9532	14.0468
	120.00	15.5000*	.000	10.4532	20.5468
96.00	24.00	-21.0000*	.000	-26.0468	-15.9532
	48.00	-15.6667*	.000	-20.7135	-10.6199
	72.00	-9.0000*	.000	-14.0468	-3.9532
	120.00	6.5000*	.008	1.4532	11.5468
120.00	24.00	-27.5000*	.000	-32.5468	-22.4532
	48.00	-22.1667*	.000	-27.2135	-17.1199
	72.00	-15.5000*	.000	-20.5468	-10.4532
	96.00	-6.5000*	.008	-11.5468	-1.4532

Zebrafish embryo viability assay (Figure 2, Table 3 and Table 4) revealed consistently higher survival rates in Group B (E3 embryo culture medium) compared to Group A (3D-printed scaffolds) at all evaluated time points. Two-way ANOVA showed a statistically significant difference between the groups ($F=41.823$, $p<0.001$), indicating higher embryo viability in the control group. A significant main effect of time was also observed ($F=126.342$, $p<0.001$), reflecting expected developmental variations in embryo survival over the incubation period. The interaction between group and time was not significant ($F=2.355$, $p=0.089$), suggesting that both groups followed a similar pattern of change over time. The relatively lower embryo viability observed in the scaffold-exposed group is acceptable and expected, as the introduction of a biomaterial into the culture system can induce mild physiological stress during early embryonic development. However, the viability values remained within the acceptable range for non-toxic materials, indicating that the 3D-printed scaffold did not elicit any severe cytotoxic response. Thus, while the E3 culture medium supported optimal survival, the scaffold-treated embryos demonstrated adequate biocompatibility suitable for further biological evaluation. Tukey's post hoc test revealed signifi-

cant differences in embryo viability between most time points ($p<0.05$), with viability at 24 hours being significantly higher than at later intervals. A gradual, time-dependent reduction in viability was observed across 48, 72, 96, and 120 hours, which is expected under *in vitro* zebrafish culture conditions due to normal developmental progression and mild physiological stress over time. The absence of any abrupt decline confirms that the scaffold exposure did not cause acute toxicity, indicating acceptable biocompatibility of the material. There were no noticeable developmental abnormalities, such as delayed hatching or abnormal movement, in both groups. Both groups exhibited differentiation of head and tail at 48 hours; good length with prominent trunk and tail development at 96 hours, and well-developed eyes, neural tube, brain, and heart with active coordinated movements by 120 hours. The absence of significant developmental abnormalities, low levels of apoptosis, and intact embryo morphology post-exposure suggests that the scaffolds do not adversely affect embryonic development or organ function, proving the non-toxic nature of these scaffolds, indicating their potential suitability for use in tissue engineering and regenerative medicine applications.

ANTIBACTERIAL ANALYSIS - DISC DIFFUSION METHOD

The antibacterial analysis revealed a concentration-dependent effect against the four strains (Figure 3, Table 4 and Table 5). Group A1 showed the least antibacterial activity across all strains, with smaller zones of inhibition, which was in contrast to Group A2, which exhibited significantly enhanced antibacterial activity, while Group C exhibited the highest activity. Pairwise comparison revealed that Group A2 had comparable antibacterial activity to that of Group C for *S. aureus* and *S. mutans*. The negligible activity exhibited by the negative control proved that the antibacterial activity noted in Groups A1 and A2 is attributed to the scaffold components. This antibacterial property of the bioprinted scaffold would aid in achieving predictable regenerative outcomes during the wound healing process and may prove as a better alternative to the traditional bone grafting options with respect to infection control.

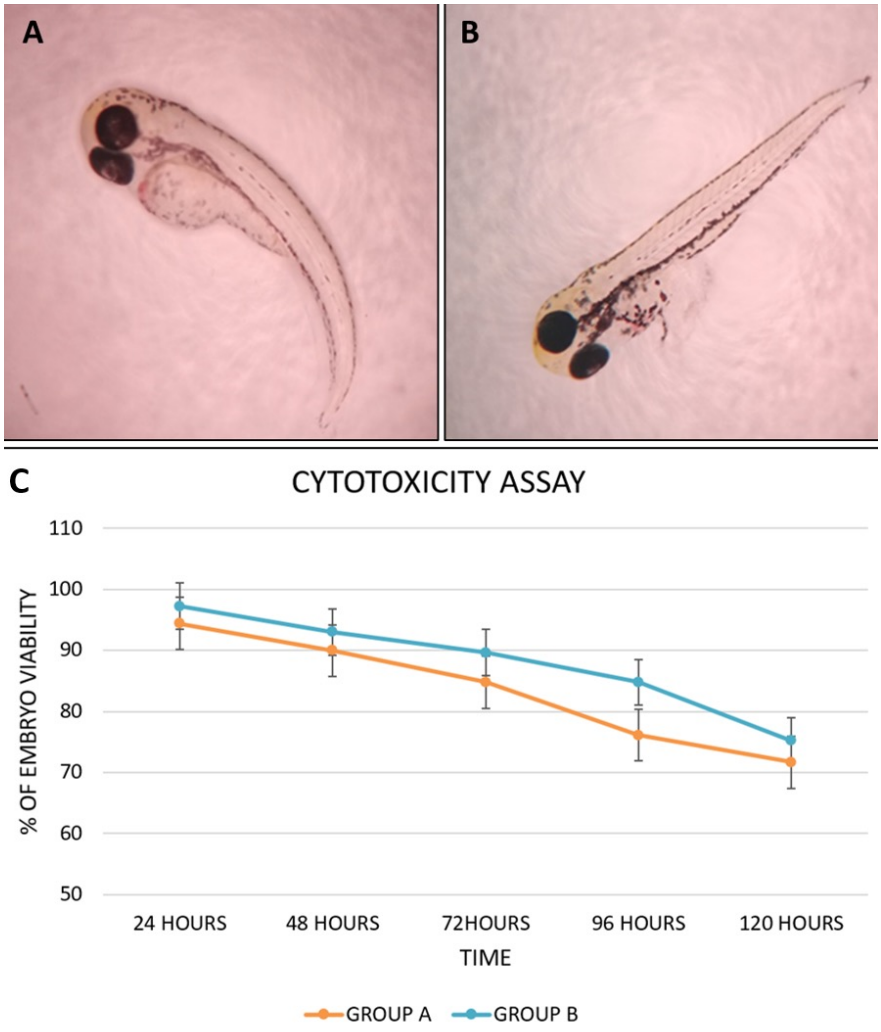

Figure 2. A-B: Cytotoxicity analysis with zebrafish model revealed good embryo development for both Groups A (A) and B (B), C: Comparative analysis of cytotoxicity of Groups A and B at various time points, expressed as percentage of embryo viability.

Table 3. Comparison of cytotoxicity as mean embryo viability (%) between Groups A and B at different time intervals using two-way ANOVA

Time (hours)	Group A (Mean ± SD)	Group B (Mean ± SD)	F (Group)	P (Group)	F (Time)	P (Time)	F (Group x Time)	P Group x Time)
24	94.44 ± 1.39	97.22 ± 0.70						
48	90.00 ± 2.00	93.00 ± 2.65						
72	84.78 ± 1.35	89.67 ± 0.58	41.823	<0.001	126.342	<0.001	2.355	0.089
96	76.11 ± 3.47	84.78 ± 1.95						
120	71.67 ± 2.08	75.22 ± 1.34						

Table 4. Tukey's post hoc comparison of cytotoxicity across time intervals.

(I) Time		Mean Difference (I-J)	Sig.	95% Confidence Interval	
				Lower Bound	Upper Bound
24.00	48.00	4.3317*	.008	.9829	7.6805
	72.00	8.6100*	.000	5.2612	11.9588
	96.00	15.3883*	.000	12.0395	18.7371
	120.00	22.3883*	.000	19.0395	25.7371
48.00	24.00	-4.3317*	.008	-7.6805	-.9829
	72.00	4.2783*	.008	.9295	7.6271
	96.00	11.0567*	.000	7.7079	14.4055
	120.00	18.0567*	.000	14.7079	21.4055
72.00	24.00	-8.6100*	.000	-11.9588	-5.2612
	48.00	-4.2783*	.008	-7.6271	-.9295
	96.00	6.7783*	.000	3.4295	10.1271
	120.00	13.7783*	.000	10.4295	17.1271
96.00	24.00	-15.3883*	.000	-18.7371	-12.0395
	48.00	-11.0567*	.000	-14.4055	-7.7079
	72.00	-6.7783*	.000	-10.1271	-3.4295
	120.00	7.0000*	.000	3.6512	10.3488
120.00	24.00	-22.3883*	.000	-25.7371	-19.0395
	48.00	-18.0567*	.000	-21.4055	-14.7079
	72.00	-13.7783*	.000	-17.1271	-10.4295
	96.00	-7.0000*	.000	-10.3488	-3.6512

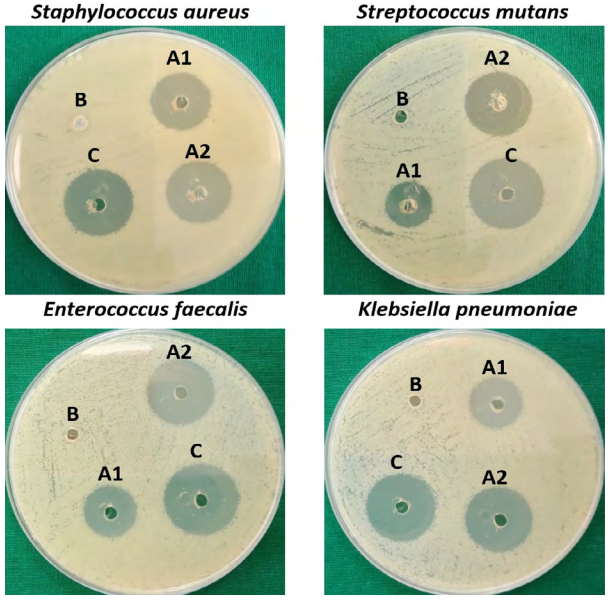

Figure 3. Antibacterial analysis of Group A1 (low concentration of 3D bioprinted scaffolds). Group A2 (high concentration of 3D bioprinted scaffolds), Group B (negative control), and Group C (positive control) against common oral pathogens.

DISCUSSION

The present study developed a novel composite bioink composed of PEGDA-PEG-HAP-COL-CH, which was used for 3D bioprinting of osseous scaffolds for bone regeneration. Biologic characterisation revealed good biocompatibility and limited cytotoxicity of the 3D bioprinted scaffolds, in comparison to untreated MG63 cells E3 embryo culture medium, respectively, which served as the control, proving that they are safe for tissue engineering applications. The presence of viable, actively motile, and proliferating cells validates that the scaffold not only maintains cell health but also promotes cellular differentiation and proliferation, underscoring its potential for regenerative applications. Similar results were observed in a study that assessed the effect of PEG on PLA scaffolds, and it showed that increasing the PEG concentration enhanced cell viability, adhesion, and osteogenic behaviour (9). Another study that assessed CH-based scaffolds enriched with HAP showed amplified apatite formation due to the presence of HAP (10). The scaffolds showed good biocompatibility with no toxicity towards rat bone marrow mesenchymal stem cells (BMSCs). Similarly, HAP-COL based bioprinted scaffolds with BMSCs in and on the scaffolds showed high cell viability, proliferation, and ALP activity (11). Another recent study stated that the osteoconductive properties of the 3D printed COL scaffolds were comparable to PEGDA scaffolds (12). The development of a composite PEG-PEGDA-HAP-COL-CH based scaffold in this study may provide a synergistic effect of its component biomaterials, exerting an enhanced regenerative outcome.

The antibacterial analysis also revealed good activity against common oral pathogens that was comparable to the antibiotic standard used. It underscores the significance of CH incorporation in the scaffolds and serves as a valuable mechanism to prevent infections at the regenerative sites. The results of this study are in accordance with other studies that assessed the antibacterial properties of CH-based scaffolds, with a similar ZOI against common oral pathogens (13). Chitosan is thought to exhibit antibacterial properties by interacting with the negatively charged bacterial cell wall, leading to cell disruption, changes in membrane permeability, and interference with DNA replication, ultimately resulting in cell death (14). Additionally, it functions as a chelating agent, promoting toxin formation and suppressing microbial growth.

A combination of PEG and PEGDA was chosen as the base of the bioink, being versatile polymers with photocrosslinkable properties. Their non-toxic, biocompatible, minimally immunogenic, hydrophilic, and tunable nature makes them suitable for tissue scaffolding and wound healing applications (15). HAP was added to provide the compositional and structural similarity to the bone, acting as mineralisation nodes, allowing for cell attachment and differentiation (16-17). The addition of COL would serve as the organic component of the scaffold, resembling the ECM of the bone tissue. The triple helix component of COL would provide strength, flexibility, and tenacity, enabling the scaffolds to withstand and dissipate the forces (18-19). Moreover, the RGD motifs of COL would get physically functionalised with the polymer network and act as a framework for osteoblastic cell attachment and mineralisation. The degradation products of COL would also act as signalling peptides for the regulation of bone turnover (20).

The incorporation of CH, a biopolymer derived from chitin, may add beneficial properties of biocompatibility, biodegradability, non-cytotoxic and non-immunogenic behaviour to the scaffolds (21,22). Its high hydrophilicity allows the scaffold surface to resemble native ECM. The positively charged surface of CH facilitates interactions with the negatively charged cell membranes, allowing for cell adhesion (23). The crosslinking of CH with other biopolymers like COL, along with the incorpo-

ration of HAP, creates an inherent 3D architecture, promoting cell spreading and migration throughout the matrix, facilitating nutrient exchange and waste removal. CH has been shown to promote the differentiation of mesenchymal stem cells (MSCs) into osteoblasts (24). The physical structure of CH scaffolds with its mechanical cues, combined with its bioactive properties, creates an optimal environment for osteogenesis (25). The material's inherent properties, like its degree of deacetylation, porosity, and surface charge, can stimulate signaling pathways involved in osteoblast differentiation, such as the Wnt/β-catenin pathway (26). Moreover, its intrinsic antimicrobial property would reduce the risk of infections during the wound healing and regenerative phase, allowing for fabrication of 3D bioprinted scaffolds with enhanced infection control. It also provides various degrees of customisation due to its tunable molecular weight and cross-linking properties, allowing for specific tailoring of the scaffolds according to the tissue. Its ability to be processed into various forms such as fibers, films, and sponges, provides versatility to the printing process.

The present study confirms the successful development of a composite bioink PEG-PEGDA-HAP-COL-CH, and the bioprinting of osseous scaffolds. Biologic characterisation revealed good biocompatibility and limited cytotoxicity of the scaffolds. The incorporation of CH allowed expression of good antibacterial activity against common oral pathogens, comparable to that of antibiotic standards. Fabrication of scaffolds with inherent antibacterial properties would not only enhance the regenerative outcomes, it may also reduce the need for high doses of antibiotics. However, the limitations of this study lie in the fact that mineralisation, gene expression, and in vivo efficacy of the scaffolds were not analysed. Further studies should focus on assessing the efficacy of these scaffolds in *in vivo* models to analyse the genetic markers and the mineralisation potential of the scaffolds. Successful clinical applications of the scaffolds would ultimately enhance the masticatory efficiency of individuals, improving their overall health and quality of life.

CONCLUSION

The need for bioengineered 3D scaffolds remains essential globally, and though various grafting options are available, 3D bioprinting provides patient-centric precision treatment strategies. The developed bioink and 3D bioprinted scaffolds demonstrated good biocompatibility, minimal cytotoxicity, and inherent antibacterial properties, supporting their use in bone regenerative applications. However, further studies evaluating mineralisation, gene expression, and in vivo performance are essential to comprehensively validate their therapeutic potential and ensure successful clinical translation.

CONFLICT OF INTEREST: None declared.

SOURCE OF FUNDING: None.

STUDY APPROVAL: Approval for the conduction of the study was obtained from the Institutional Scientific Review Board with approval number: SRB/SDC/UG-2033/24/PERIO/470.

AUTHOR CONTRIBUTION STATEMENT: Conceptualization and design: P.A., D.S., K.G., R.B.; Literature review: P.A., K.G., R.B.; Methodology and validation: P.A.,K.G., R.B.; Formal analysis: P.A., K.G., R.B.; Investigation and data collection: P.A., D.S., K.G.; Resources: P.A., D.S., K.G., R.B.; Data analysis and interpretation: P.A., D.S., K.G., R.B.; Writing-original draft preparation: P.A., D.S.; Writing-review & editing: P.A., K.G., R.B.; Supervision: P.A., K.G., R.B.; Project administration: P.A., D.S., K.G., R.B.; Funding acquisition: P.A., D.S., K.G., R.B.

ACKNOWLEDGEMENT: The authors gratefully acknowledge the Department of Chemical Engineering, Indian Institute of Technology, Madras, for providing access to their 3D bioprinting facilities and technical support throughout the study.

REFERENCES

1. Bishop E.S., Mostafa S., Pakvasa M., Luu H.H., Lee M.J., Wolf J.M., et al. 3-D bioprinting technologies in tissue engineering and regenerative medicine: Current and future trends. Genes Dis. 2017; 4 (4): 185-195.
2. Arumugam P., Kaarthikeyan G., Eswaramoorthy R. Three-Dimensional Bioprinting: The Ultimate Pinnacle of Tissue Engineering. Cureus. 2024; 16 (4): e58029.
3. Ramesh S., Harrysson O., Rao P., Tamayol A., Cormier D., Zhang Y., et al. Extrusion bioprinting: Recent progress, challenges, and future opportunities. Bioprinting. 2021; 21: e00116.
4. Chen X.B., Anvari-Yazdi F., Duan X., Zimmerling A., Gharraei R., Sharma N.K., et al. Biomaterials / bioinks and extrusion bioprinting. Bioact Mater. 2023; 28: 511-536.
5. Gungor-Ozkerim P.S., Inci I., Zhang Y.S., Khademhosseini A., Dokmeci M.R. Bioinks for 3D bioprinting: an overview. Biomater Sci. 2018; 6 (5): 915-946.
6. Krishna D.V., Sankar M.R. Persuasive factors on the bioink printability and cell viability in the extrusion-based 3D bioprinting for tissue regeneration applications. Engineered Regeneration. 2023; 4: 396-410.
7. Reddy M.S.B., Ponnamma D., Choudhary R., Sadasivuni K.K. A Comparative Review of Natural and Synthetic Biopolymer Composite Scaffolds. Polymers (Basel). 2021; 13 (7): 1105.
8. Zhang J., Wehrle E., Rubert M., Müller R. 3D Bioprinting of Human Tissues: Biofabrication, Bioinks, and Bioreactors. Int J Mol Sci. 2021; 22 (8): 3971.
9. Salehi S., Ghomi H., Hassanzadeh-Tabrizi S.A., Koupaei N., Khodaei M. The effect of polyethylene glycol on printability, physical and mechanical properties and osteogenic potential of 3D-printed poly (l-lactic acid)/ polyethylene glycol scaffold for bone tissue engineering. Int J Biol Macromol. 2022; 221: 1325-1334.
10. Yousefiasl S., Sharifi E., Salahinejad E., Makvandi P., Irani S. Bioactive 3D-printed chitosan-based scaffolds for personalized craniofacial bone tissue engineering. Engineered Regeneration. 2023; 4: 1-11.
11. Guo C., Wu J., Zeng Y., Li H. Construction of 3D bioprinting of HAP/collagen scaffold in gelation bath for bone tissue engineering. Regen Biomater. 2023; 10: rbad067.
12. Kontakis M.G., Moulin M., Andersson B., Norein N., Samanta A., Stelzl C., et al. Trabecular-bone mimicking osteoconductive collagen scaffolds: an optimized 3D printing approach using freeform reversible embedding of suspended hydrogels. 3D Print Med. 2025; 11 (1): 11.
13. Salehi S., Ghomi H., Hassanzadeh-Tabrizi S.A., Koupaei N., Khodaei M. Antibacterial and osteogenic properties of chitosan-polyethylene glycol nanofibre-coated 3D printed scaffold with vancomycin and insulin-like growth factor-1 release for bone repair. Int J Biol Macromol. 2025; 298: 139883.
14. Atay H.Y. Antibacterial Activity of Chitosan-Based Systems. Functional Chitosan. 2020; 457-89.
15. Zhu J. Bioactive modification of poly(ethylene glycol) hydrogels for tissue engineering. Biomaterials. 2010; 31 (17): 4639-56.
16. Ielo I., Calabrese G., De Luca G., Conoci S. Recent Advances in Hydroxyapatite-Based Biocomposites for Bone Tissue Regeneration in Orthopedics. Int J Mol Sci. 2022; 23 (17): 9721.
17. Sharon V.M., Malaiappan S. Biocompatibility and periodontal regenerative potential of hydroxyapatite nanoparticles from Portunus

Sanguinolentus Shells: A crystallographic, morphological, and molecular gene expression analysis. J Dent. 2025; 157: 105762.
18. Fidler A.L., Boudko S.P., Rokas A., Hudson B.G. The triple helix of collagens - an ancient protein structure that enabled animal multicellularity and tissue evolution. J Cell Sci. 2018; 131 (7): jcs203950.
19. Selvaraj V., Sekaran S., Dhanasekaran A., Warrier S. Type 1 collagen: Synthesis, structure and key functions in bone mineralization. Differentiation. 2024; 136: 100757.
20. Seibel M.J. Biochemical markers of bone turnover: part I: biochemistry and variability. Clin Biochem Rev. 2005; 26 (4): 97-122.
21. Pramanik S., Aggarwal A., Kadi A., Alhomrani M., Alamri A.S., Alsanie W.F., et al. Chitosan alchemy: transforming tissue engineering and wound healing. RSC Adv. 2024; 14 (27): 19219-19256.
22. Vaidya G., Pramanik S., Kadi A., Rayshan A.R., Abualsoud B.M., Ansari M.J., et al. Injecting hope: chitosan hydrogels as bone regeneration innovators. J Biomater Sci Polym Ed. 2024; 35 (5): 756-797.
23. Kim Y., Zharkinbekov Z., Raziyeva K., Tabyldiyeva L., Berikova K., Zhumagul D., et al. Chitosan-Based Biomaterials for Tissue Regeneration. Pharmaceutics. 2023; 15 (3): 807.
24. Kudiyarasu S., Karuppan Perumal M.K., Rajan Renuka R., Manickam Natrajan P. Chitosan composite with mesenchymal stem cells: Properties, mechanism, and its application in bone regeneration. Int J Biol Macromol. 2024; 275 (Pt 1): 133502.
25. Aguilar A., Zein N., Harmouch E., Hafdi B., Bornert F., Offner D., et al. Application of Chitosan in Bone and Dental Engineering. Molecules. 2019; 24 (16): 3009.
26. Oh Y., Ahn C.B., Marasinghe M.P.C.K., Je J.Y. Insertion of gallic acid onto chitosan promotes the differentiation of osteoblasts from murine bone marrow-derived mesenchymal stem cells. Int J Biol Macromol. 2021; 183: 1410-1418.